Calculation of Low Reynolds Number Flows at High Angles of Attack

T. Cebeci,* M. McIlvaine,† and H. H. Chen‡
California State University, Long Beach, California 90840
and
R. H. Liebeck§
Douglas Aircraft Company, Long Beach, California 90846

Calculated results are reported for Eppler and Liebeck airfoils with chord Reynolds numbers ranging from 10^5 to 5×10^5 and for angles of attack up to stall. They were obtained with an interactive finite-difference boundary-layer method in which the turbulence model employs an extended intermittency expression in the Cebeci and Smith eddy-viscosity model and the location of the onset of transition is determined from linear-stability theory. Comparisons with experiments indicate agreement within measurement uncertainty, except at stall conditions, and close correspondence with the ISES code, which is based on the solution of integral equations.

I. Introduction

In recent years the subject of low Reynolds number airfoils has received considerable interest in both civil and military applications including remotely piloted vehicles, propeller and wind turbine aerodynamics, aircraft with high-aspect ratio wings, and ultralight human-powered vehicles, as evidenced in a review article by Lissaman,[1] two proceedings volumes edited by Mueller,[2,3] and one by the Royal Aeronautical Society.[4] The behavior of these airfoils differs from those at high Reynolds numbers in that rather large separation bubbles can occur some way downstream of the leading edge with transition taking place within the bubble prior to reattachment. The length of the bubble increases with a decreasing Reynolds number and strongly influences the performance characteristics of the airfoils.

As at high Reynolds numbers, the performance characteristics of airfoils can be predicted by methods based either on the solution of the Navier-Stokes equations or on a combination of inviscid and boundary-layer equations. In both approaches, the accuracy of the method depends on the numerical method, the turbulence model, and the method used to compute the location of the onset of transition. The differences between calculation methods for high and low Reynolds numbers are mainly in the prediction of the transition location and in the modeling of the transition region. When the Reynolds number is high, the onset of transition occurs before or at the flow separation point, and the extent of the transition region is confined to a relatively small region. When transition occurs before laminar separation, it can be computed by correlation formulas such as those suggested by Michel[5] and Granville[6] or by the e^n method based on linear stability theory, as suggested by Smith[7] and van Ingen.[8] Several turbulence models, mostly developed for attached flows, can be used to model the transition region[9]; models suggested by Dhawan and Narasimha[10] and Chen and Thyson[11] are popular. Except at very high angles of attack where the flow corresponds to stall or post-stall conditions, these methods and models are often satisfactory in predicting airfoil flows, as discussed in Refs. 12 and 13. With decreasing Reynolds number, however, rather large separation bubbles begin to appear on the airfoil; the onset of transition occurs inside the bubble and is separation induced. The importance of the turbulence model for the transition region increases and plays a bigger role in the computational method. As a result, the methods used to predict airfoil characteristics at low Reynolds numbers must be modified to account for these phenomena, which are either absent or not important at high Reynolds number flows.[14-17]

The present paper addresses the two essential ingredients that must be included in any theoretical method for predicting the performance of low Reynolds number airfoils, regardless of the approach used to solve the conservation equations. The proposed ingredients are included in the inviscid-viscous interactive finite-difference method reported in Ref. 17, which is briefly described in the following section, with special emphasis on the model used to represent the transitional flow and the method used to calculate the onset of transition. In Sec. 3, the predictions of this method together with an integral method due to Drela and Giles[15] are compared with experimental data for several airfoils at low and high angles of attack and for chord Reynolds numbers ranging from 10^5 to 5×10^5. The paper ends with a summary of the more important findings.

II. Inviscid/Viscous Interactive Method

The interactive method is described for high and low Reynolds numbers in Refs. 12 and 17, respectively, and makes use of the conformal mapping method of Halsey[18] coupled to an inverse finite-difference boundary-layer method of Cebeci[19] that makes use of the interactive formula suggested by Veldman.[20] The conformal mapping involves transformation of the region outside the airfoil to the region outside of a unit circle and solution of the resulting equations in the transformed plane. The transformation is achieved in a sequence of three conformal mappings and the solutions of the transformed equations, which include the flow on the airfoil and in the wake and make use of Fourier-analysis techniques discussed in Ref. 12. The Reynolds shear stress term in the boundary-layer equations is expressed in terms of an eddy

Received Dec. 11, 1989; presented as Paper 90-0569 at the AIAA 28th Aerospace Sciences Meeting, Reno, NV, Jan 8-11, 1990; revision received and accepted for publication Aug. 6, 1990.

*Professor and Chairman, Aerospace Engineering Department. Fellow AIAA.
†Graduate Student, Aerospace Engineering Department. Member AIAA.
‡Associate Professor, Aerospace Engineering Department. Member AIAA.
§MDC Fellow, Government Program Development. Fellow AIAA.

viscosity ϵ_m, and the resulting equations are solved subject to the usual boundary conditions with the external velocity $u_e(x)$ expressed as the sum of inviscid velocity $u_e^0(x)$ and a perturbation velocity $\delta u_e(x)$ computed from the Hilbert integral

$$\delta u_e(x) = \frac{1}{\pi} \int_{x_a}^{x_b} \frac{\mathrm{d}}{\mathrm{d}\sigma} (u_e \delta^*) \frac{\mathrm{d}\sigma}{x-\sigma} \tag{1}$$

with the interaction region confined to (x_a, x_b). The solutions of the equations include the flow on the airfoil and in the wake. The eddy-viscosity formulation of Cebeci and Smith[21] is used with special emphasis on the transitional region

$$\epsilon_m = \begin{cases} \epsilon_{m_i} = L^2 \left| \dfrac{\partial u}{\partial y} \right| \gamma_{\mathrm{tr}} & \text{(2a)} \\ \epsilon_{m_0} = 0.0168 u_e \delta^* \gamma_{\mathrm{tr}} & \text{(2b)} \end{cases}$$

where L and γ_{tr} are given by

$$L = 0.4y[1-\exp(-y/A)], \qquad A = 26\nu u_\tau^{-1} \tag{3a}$$

$$u_\tau = \left(\nu \frac{\partial u}{\partial y} \right)_{\max}^{1/2} \tag{3b}$$

$$\gamma_{\mathrm{tr}} = 1 - \exp\left[-G(x-x_{\mathrm{tr}}) \int_{x_{\mathrm{tr}}}^{x} \frac{\mathrm{d}x}{u_e} \right] \tag{3c}$$

Here γ_{tr} corresponds to the expression suggested by Chen and Thyson[11] with x_{tr} denoting the location of the beginning of transition and G a parameter defined by

$$G = \left(\frac{3}{C^2} \right) \frac{u_e^3}{\nu^2} R_{x_{\mathrm{tr}}}^{-1.34} \tag{4}$$

where the transition Reynolds number $R_{x_{\mathrm{tr}}} = (u_e x/\nu)_{\mathrm{tr}}$ and C is constant with a recommended value of 60. In Ref. 17, the Chen and Thyson model was modified to include low Reynolds numbers with separation. A correlation formula, shown in Fig. 1, was devised to represent C^2 of Eq. (4) in terms of $R_{x_{\mathrm{tr}}}$ for the experimental data obtained for airfoils NACA 66_3-018, ONERA D, NACA 65-213, and LNV109A. The data encompass a Reynolds number range from $R_c = 2.4 \times 10^5$ to 2×10^6, and fall conveniently on a straight line on a semilog scale represented by the equation

$$C^2 = 213\ [\log R_{x_{\mathrm{tr}}} - 4.7323] \tag{5}$$

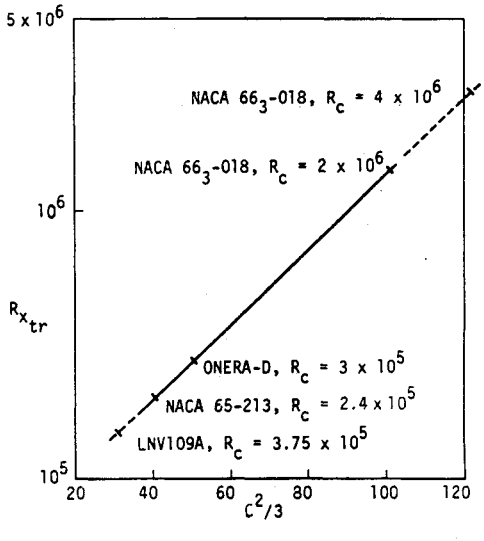

Fig. 1 Variation of $C^2/3$ with transition Reynolds number.

For the wake flow calculations following the study of Chang et al.,[22] the eddy-viscosity formulation for wall boundary-layer formulas was modified and expressed in the form

$$\epsilon_m = (\epsilon_m)_w + [(\epsilon_m)_{te} - (\epsilon_m)_w] \exp\left[\frac{x_{te}-x}{20\delta_{te}} \right] \tag{6}$$

where $(\epsilon_m)_w$ denotes the eddy viscosity for the far wake given by the maximum of $(\epsilon_m)_w^\ell$ and $(\epsilon_m)_w^u$ defined by

$$(\epsilon_m)_w^\ell = 0.064 \int_{-\infty}^{y_{\min}} (u_e - u)\, \mathrm{d}y \tag{7a}$$

$$(\epsilon_m)_w^u = 0.064 \int_{y_{\min}}^{\infty} (u_e - u)\, \mathrm{d}y \tag{7b}$$

with $y_{\min}$ denoting the location where $u = u_{\min}$.

The location of transition was determined from the e^n-method. At first, the laminar and turbulent boundary-layer calculations were performed on the airfoil and in the wake for a transition location computed by Michel's methods and an inviscid pressure distribution. Next, laminar flow calculations were carried out on the airfoil to obtain the velocity profiles needed in the solution of the Orr-Sommerfeld equation. The stability calculations were then initiated at a chordwise location where the displacement-thickness Reynolds number exceeded its critical value established for similar boundary layers.[17] For a dimensional frequency ω^* determined at say $x = x_0$, the amplification rates α_i were computed along the airfoil in order to evaluate the integral

$$n = \int_{x_0}^{x} -\alpha_i \, \mathrm{d}x \tag{8}$$

so that the location of transition could be determined from the e^n method. This process was repeated for different values of ω^* to obtain similar integrated amplification rates. As discussed by Cebeci and Egan,[23] the envelope procedure used to calculate the critical frequency that leads to the most amplified disturbance is not applicable for flows with separation as in three-dimensional flows, and it was necessary to search for this frequency in the calculations. Since with separation the velocity profiles change significantly from those of attached flows, the amplification rates became sensitive to the dimensional frequencies and required implementation of the eigenvalue procedure used in the solution of the Orr-Sommerfeld equation. This was done, as discussed in Ref. 17, by the use of a continuation method.

Once transition had been determined with this procedure, a new set of laminar boundary-layer calculations were performed until the transition location, after which the turbulent flow calculations were performed on the airfoil and in the wake. The displacement-thickness distribution resulting from these calculations was used to determine a blowing velocity v_n by differentiating the product of external velocity and displacement thickness with respect to the surface distance so that the inviscid flow equations were solved again subject to a new boundary condition. This process was repeated on an iterative basis until the solutions of boundary-layer, stability, and inviscid-flow equations converged.

III. Results and Discussion

In the study conducted in Ref. 17, the accuracy of the method described in the preceding section was evaluated for five separate airfoils with chord Reynolds numbers ranging from 3×10^5 to 8×10^6. Except for one airfoil, the range of angle of attack was limited to small values. The study showed that, with a combination of the e^n method and a modified transitional model in the Cebeci-Smith algebraic eddy-viscosity formulation, the lift and drag coefficients could be calculated accurately.

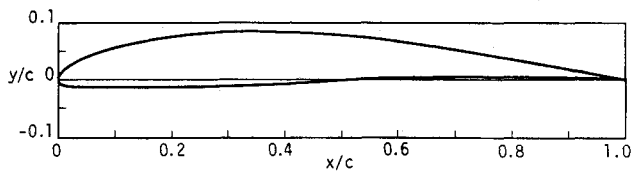

Fig. 2 Eppler 387 airfoil.

In the present study, we consider the airfoils due to Eppler and Liebeck and perform calculations for chord Reynolds numbers ranging from 10^5 to 5×10^5 and for angles of attack up to stall. For the Eppler airfoil, we compare the predictions of our method with the experimental data of McGhee et al.[24] and for the Liebeck airfoils with experiments conducted in the Douglas wind tunnel and with the predictions of a method due to Drela and Giles.[15] In this method, the steady Euler equations were used in integral form to represent the inviscid flow and a compressible lag-dissipation integral method used to represent the boundary layers and wakes. The inviscid and viscous flow solutions were coupled through the displacement thickness and the onset of transition computed by an e^n type of method. Rather than solving the nonsimilar boundary layers, as in the method of Sec. II, this method made use of a modified procedure developed by Gleyzes et al.[25] in which the Orr-Sommerfeld equation was solved with velocity profiles based on the solution of the Falkner-Skan equation. Additional details are provided in Ref. 15.

A. Results for the Eppler Airfoil

The experimental data of McGhee et al.[24] contain measurements for the Eppler airfoil (see Fig. 2) in the Langley Low-Turbulence Pressure Tunnel (LTPT). The tests were conducted over a Mach number range from 0.03 to 0.13 and a chord Reynolds number range from 60×10^3 to 460×10^3. Lift and pitching-moment data were obtained from airfoil surface pressure measurements and drag data from wake surveys. Oil flow visualization was used to determine laminar-separation and turbulent-reattachment locations.

The calculations for the Eppler airfoil were performed for chord Reynolds numbers of 10^5, 3×10^5, and 4.6×10^5 and for a range of angles of attack up to stall. Since the Reynolds number range of the present study is less than that of Fig. 1, which led to the expression given by Eq. (5), studies were first conducted to investigate the influence of the $C^2/3$ parameter at the Reynolds number of 1×10^5. It was found that values of $C^3/3$ from 10 to 30 led to negligible differences in the lift coefficient and differences of less than 3% in the drag coefficient. Thus, the straight-line formulation of Fig. 1 appears to be valid at a chord Reynolds number of 1×10^5, and the calculation of the transition-region flow is adequate.

The calculation method of Sec. II requires the coordinates of the airfoil, the chord Reynolds number, and a value of n for the e^n method, which, in a way, represents the effect of freestream turbulence on transition and is given by

$$n = -8.43 - 2.4 \ln T \tag{9}$$

where

$$T = \sqrt{u'^2/u_e} \tag{10}$$

as proposed by Mack.[26] According to Ref. 24, the measured turbulence level was 0.06% for a total pressure $p_t = 15$ psi, which, according to Eq. (9), corresponds to a value of $n = 9.4$ and was used in all of the Eppler airfoil calculations except for those at $R_c = 1 \times 10^5$. Studies at this Reynolds number showed that with $n = 12$, the calculated pressure coefficient C_p distributions were in better agreement with data than those with $n = 9.4$.

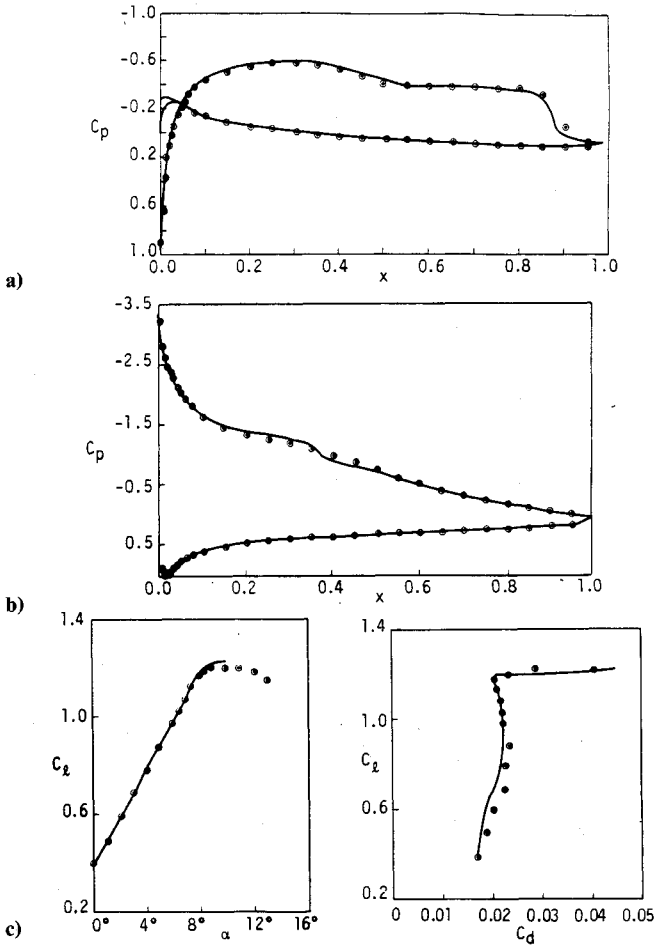

Fig. 3 Comparison of calculated (solid lines) and measured (symbols) pressure-coefficient distributions at a) $\alpha = 0$ deg; b) $\alpha = 8$ deg; and c) lift and drag coefficients for $R_c = 1 \times 10^5$ with $n = 12$.

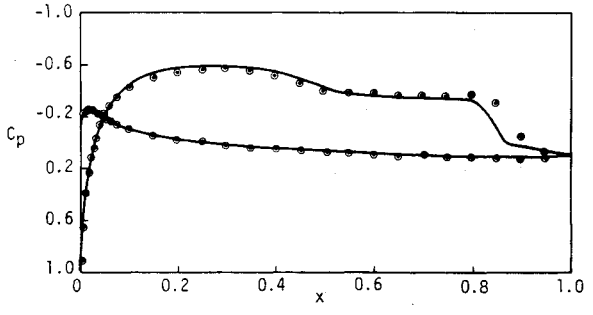

Fig. 4 Comparison of calculated (solid lines) and measured (symbols) pressure-coefficient distributions of the Eppler airfoil at $\alpha = 0$ deg, $R_c = 1 \times 10^5$, $n = 9.4$.

Figures 3a and 3b allow comparison between measured and calculated distributions of pressure coefficients for angles of attack of 0 and 8 deg, respectively, and Fig. 3c allows comparison between measured and calculated lift and drag coefficients for $R_c = 1 \times 10^5$, all computed with $n = 12$. Figure 4 presents similar results to those in Fig. 3a with $n = 9.4$ and indicates that a higher value of n allows the calculations to capture better the constant values of pressure coefficient associated with the separation bubble but does not influence the flow in the leading-edge region; in both cases, the calculated results are nearly the same and deviate only slightly from experiment in the immediate vicinity of the leading edge where the gradient of the pressure coefficient changes sign rapidly.

Figures 5 and 6 allow similar comparisons for Reynolds numbers of 3×10^5 and 4.6×10^5 with stability/transition calculations performed with $n = 9.4$. The agreement between the

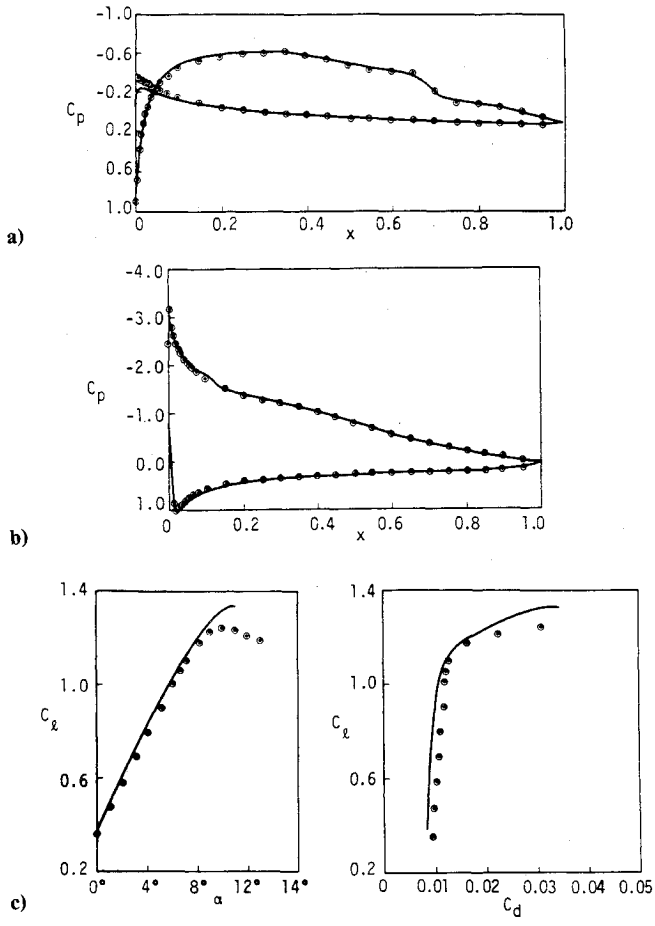

Fig. 5 Comparison of calculated (solid lines) and measured (symbols) pressure-coefficient distributions at a) $\alpha = 0$ deg; b) $\alpha = 8$ deg; and c) lift and drag coefficients for $R_c = 3 \times 10^5$.

calculated and measured distributions of pressure coefficients for angles of attack of 0 and 8 deg is similar to that in Fig. 3 for $R_c = 1 \times 10^5$. In general, the agreement is very good except in the leading-edge region for zero angle of attack.

The calculated lift and drag coefficients for the three chord Reynolds numbers of Figs. 3c, 5c, and 6c indicate remarkably good agreement with experiment for all angles of attack up to stall. There, the computed lift coefficients begin to deviate from data, indicating higher values than those measured; the discrepancy increases with an increase in Reynolds number, and the solutions do not follow the poststall behavior. We believe the reason for this discrepancy lies in the transition-calculation procedure; with an increasing angle of attack, the onset of transition on the upper surface of the airfoil moves upstream, and near stall conditions take place almost at the leading edge. Consistent with the studies of Ref. 13, a very slight change in the transition location has a large influence on the lift and drag coefficients. Moving the transition location downstream of the calculated value increases the region of flow separation and decreases the lift coefficient in accord with experiment, but, in some cases, it also causes the calculations to break down. To improve the calculations near stall and to extend them to poststall flows, it was necessary to implement the present calculation method with procedures similar to those devised for high Reynolds number airfoils described in Ref. 13. These studies are in progress and will be reported separately.

Further details of the results shown in Figs. 3–6 are presented in Tables 1 and 2. The calculated values of the chordwise location of laminar separation (LS), turbulent reattachment (TR), and the onset of transition are given in Table 1 for several angles of attack. The experimental results of this table are subject to some uncertainty because of difficulties associated with the surface visualization technique. With this proviso, comparison between measured and calculated values must be considered outstanding. It should be noted that when there is a separation bubble, the transition location obtained from the e^n method occurs within the bubble in all cases, and, in accord with experimental observation, leads to reattachment some distance downstream.

The lift and drag coefficients obtained for three Reynolds numbers are listed in Table 2 for several angles of attack together with the experimental results obtained in the Stuttgart and Langley wind tunnels and the predictions from the Eppler code included in Ref. 24. In general, our calculated lift and drag coefficients are in good agreement with Langley data. It is interesting to note that the results of the Eppler code, which contains different and more limited assumptions than the present method, provides similar results at these angles of attack, although its drag predictions are not as good as those computed with the present method at very low Reynolds numbers.

B. Results for the Liebeck Airfoils

Calculations for two Liebeck airfoils designated as LTR201 and LTR217 were performed for chord Reynolds numbers of 2.5×10^5 and 5×10^5 and for a range of angles of attack up to stall. These two airfoils were developed several years ago using the Douglas/Liebeck design method, which is based on a roof-top plus Stratford pressure recovery distribution. These are relatively early low Reynolds number designs, and they lack refinement of the transition region of the upper surface pressure distribution. The airfoils represent two distinct phi-

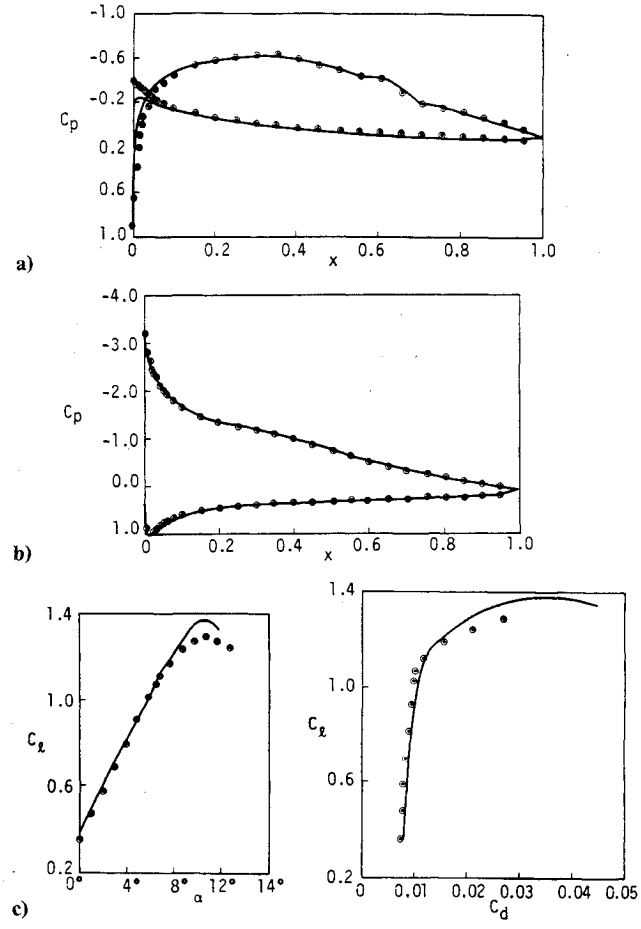

Fig. 6 Comparison of calculated (solid lines) and measured (symbols) pressure-coefficient distributions at a) $\alpha = 0$ deg; b) $\alpha = 8$ deg; and c) lift and drag coefficients for $R_c = 4.60 \times 10^5$.

Table 1 Experimental and calculated chordwise laminar separation (LS), and turbulent reattachment (TR), and transition locations on the upper surface of the Eppler airfoil.

	Experiment		$\left(\frac{x}{c}\right)_{tr}$	Calculated	
α, deg	LS	TR		LS	TR
$R_c = 1\times10^5$ ($n = 12$)					
0	0.45	0.87	0.78	0.49	0.89
2	0.41	0.79	0.70	0.44	0.82
4	0.35	0.73	0.64	0.39	0.76
5	0.34	0.67	0.60	0.37	0.70
6	0.33	0.62	0.565	0.34	0.66
$R_c = 1\times10^5$ ($n = 9.4$)					
0	0.45	0.87	0.76	0.50	0.87
2	0.41	0.79	0.68	0.45	0.79
4	0.35	0.73	0.62	0.40	0.73
5	0.34	0.67	0.585	0.38	0.69
6	0.33	0.62	0.54	0.35	0.64
$R_c = 3\times10^5$					
0	0.48	0.69	0.63	0.51	0.72
2	0.45	0.62	0.58	0.46	0.67
4	0.40	0.58	0.52	0.43	0.60
5	0.39	0.55	0.49	0.415	0.57
6	0.38	0.50	0.43	0.42	0.50
6.5	0.38	0.44	0.40	0.41	0.46
$R_c = 4.6\times10^5$					
0			0.61	0.51	0.68
2			0.56	0.48	0.62
4	No Data		0.50	0.44	0.55
5			0.45	0.44	0.49
6			0.36	—	—

Table 2 Measured and calculated values of lift and total drag coefficients

	Stuttgart experiments		Langley experiments		Eppler code		Present method	
α, deg	C_ℓ	C_d	C_ℓ	C_d	C_ℓ	C_d	C_ℓ	C_d
$R_c = 1\times10^5$							($n = 9.4$)	
0	0.320	0.0207	0.390	0.0167	0.393	0.0122	0.402	0.0164
2	0.520	0.0216	0.587	0.0203	0.611	0.0131	0.598	0.0189
4	0.700	0.0208	0.778	0.0230	0.795	0.0146	0.793	0.0218
5	0.780	0.0206	0.873	0.0237	0.892	0.0157	0.892	0.0221
6	0.860	0.0203	0.974	0.0224	0.960	0.0169	0.989	0.0228
$R_c = 3\times10^5$							($n = 9.4$)	
0			0.352	0.0087	0.393	0.0081	0.380	0.0078
2			0.573	0.0099	0.613	0.0086	0.604	0.0085
4	No Data		0.792	0.0109	0.833	0.0095	0.825	0.0094
5			0.901	0.0114	0.943	0.0104	0.933	0.0099
6			1.009	0.0118	1.051	0.0113	1.041	0.0105
$R_c = 4.6\times10^5$							($n = 9.4$)	
0			0.356	0.0073	0.393	0.0070	0.383	0.0078
2			0.580	0.0078	0.613	0.0075	0.607	0.0085
4	No Data		0.803	0.0090	0.833	0.0083	0.830	0.0094
5			0.914	0.0093	0.943	0.0090	0.939	0.0099
6			1.022	0.0101	1.053	0.0098	1.044	0.0105

losophies in their design: airfoil LTR201 is a conventional design with the Stratford pressure recovery terminating smoothly to the trailing-edge pressure, and airfoil LTR217 is an aft-loaded design where the Stratford recovery is followed by a short but severe pressure rise at the trailing edge. Geometry and design pressure distributions of the airfoils are given in Figs. 7a and 7b.

Figures 8 and 9 present the measured lift and drag coefficients of the two airfoils together with the calculated results obtained with the present method with n corresponding to 8

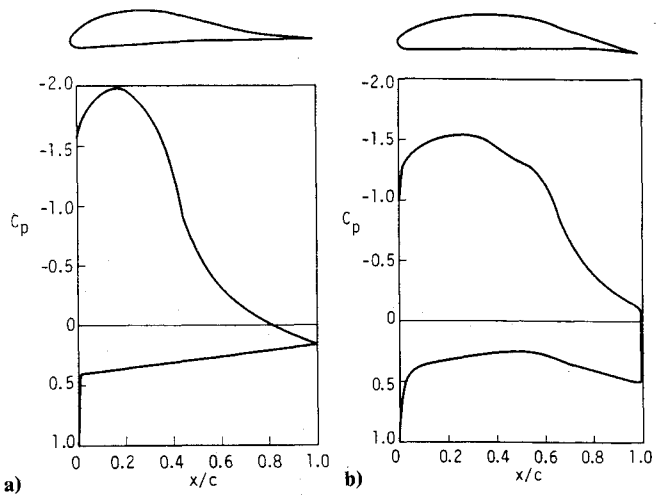

Fig. 7 Geometry and design pressure-coefficient distributions of two Liebeck airfoils: a) LTR201, $(c_\ell)_{design} = 1.16$; b) LTR217, $(c_\ell)_{design} = 1.38$.

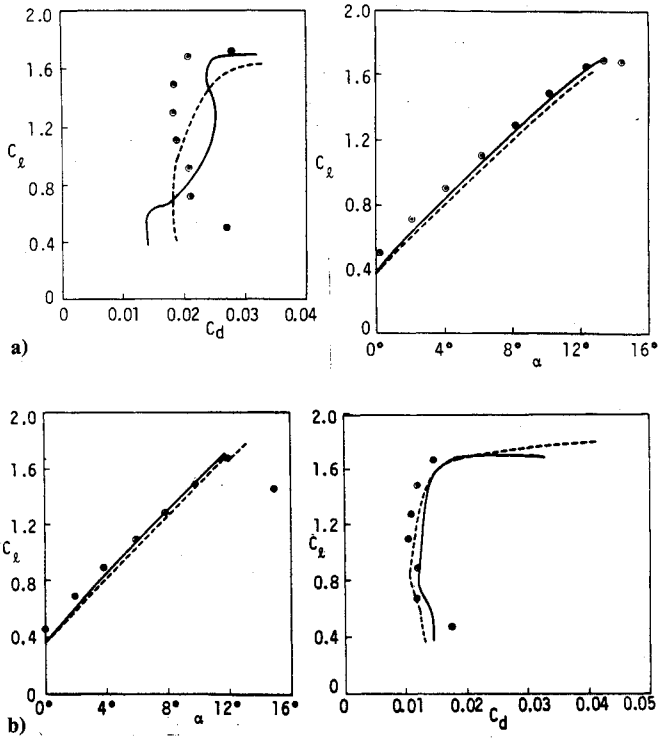

Fig. 8 Comparison of calculated (dashed lines—present method, solid lines—ISES code) and measured (symbols) lift and drag coefficients of LTR201 airfoil at a) $R_c = 2.5\times10^5$; b) $R_c = 5\times10^5$.

and with the ISES code with n corresponding to 9. Overall agreement of drag polar and lift prediction is good except for the case of airfoil LTR201 at a Reynolds number of 2.5×10^5 where both theoretical methods overestimate the effect of the laminar separation bubble and lead to less accurate drag coefficients.

These early Liebeck airfoils have performance characteristics which are sensitive to the location of laminar separation due to the nature of its surface pressure distribution. Unlike the Eppler airfoil, which has a separation bubble on its upper surface only, both Liebeck airfoils have separation bubbles on their upper and lower surfaces at very low angles of attack. This causes difficulties in the calculation procedure and, in the case of ISES code, does not allow the calculations to be

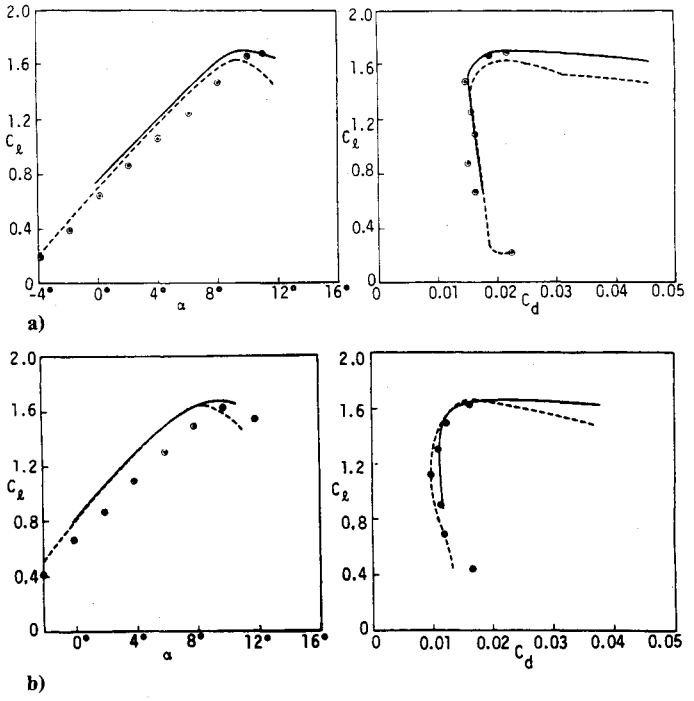

Fig. 9 Comparison of calculated (dashed lines—present method, solid lines—ISES code) and measured (symbols) lift and drag coefficients of LTR217 airfoil at a) $R_c = 2.5 \times 10^5$; b) $R_c = 5 \times 10^5$.

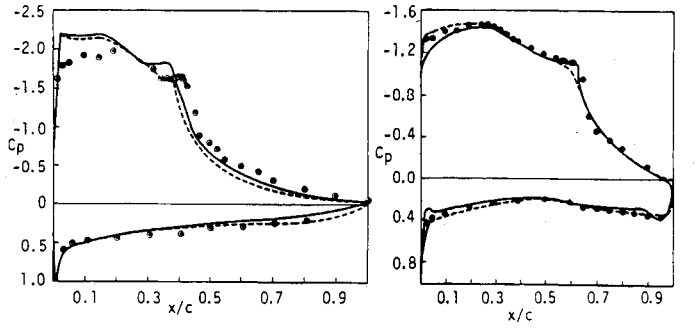

Fig. 10 Comparison of calculated (dashed lines—present method, solid lines—ISES code) and measured (symbols) pressure-coefficient distributions of a) LTR201, $(c_\ell)_{design} = 1.2$; and b) LTR217, $(c_\ell)_{design} = 1.3$, airfoils at $R_c = 2.5 \times 10^5$.

performed for angles of attack less than 0 deg for the LTR217 airfoil. It is interesting to note that the calculation times of both methods are essentially the same.

Figures 10a and 10b allow comparison between measured and calculated distributions of pressure coefficient of the two airfoils at a chord Reynolds number of 2.5×10^5. In both cases, the calculations were made by matching the experimental lift coefficient with the computed value. The results in Fig. 10a are for the LTR201 airfoil at a lift coefficient of 1.30 and indicate that, while the predicted lower surface pressure distributions are in good agreement with data, those for the upper surface are not. Both methods do not predict the distribution near the leading edge and do not capture the constant values of pressure coefficient in the separation region. Once the flow reattaches, however, the predictions of both methods improve and show better agreement with data. The results in Fig. 10b, which are for the LTR217 airfoil at a lift coefficient of 1.23, on the other hand, show good agreement with data.

IV. Concluding Remarks

In this paper, a finite-difference interactive boundary-layer method coupled with a transition prediction method based on the e^n method was applied to an Eppler airfoil and two Liebeck airfoils for chord Reynolds numbers ranging from 1×10^5 to 5×10^5 and angles of attack up to stall. In the case of Liebeck airfoils, the calculated results are also compared with the predictions of the ISES code, which employs an integral interactive boundary-layer method and a correlation based on the e^n method to predict transition. The study indicates that the finite-difference method with two essential ingredients that need to be included in any theoretical method for predicting the performance of airfoils at low Reynolds numbers, regardless of the approach used to solve the conservation equations, is able to predict the lift and drag characteristics accurately except near stall conditions.

References

[1]Lissaman, P. B. S., "Low-Reynolds-Number Airfoils," *Annual Review of Fluid Mechanics*, Vol. 15, 1983, pp. 223–239.

[2]Mueller, T. J. (ed.), *Proceedings of the Conference on Low Reynolds Number Airfoil Performance*, UNDASS-CP-77B123, June 1985.

[3]Mueller, T. J. (ed.), *Proceedings of the Conference on Low Reynolds Number Aerodynamics*, Univ. of Notre Dame, South Bend, IN, June 1989.

[4]*Proceedings of the International Conference on Aerodynamics at Low Reynolds Numbers*, The Royal Aeronautical Society, Oct. 1986.

[5]Michel, R., "Etude de la Transition sur les Profiles d'Aile; Establisement d'un Critere de Determination de Point de Transition et Calcul de la Trainee de Profile Incompressible," ONERA Rept. 1/1578A, 1951.

[6]Granville, P. S. S., "The Calculation of the Viscous Drag of Bodies of Revolution," David W. Taylor Model Basin, Washington, DC, Rept. 849, 1953.

[7]Smith, A. M. O., "Transition, Pressure Gradient, and Stability Theory," *Proceedings of the IX International Congress of Applied Mechanics*, Brussels, Vol. 4, 1956, pp. 234–244.

[8]Van Ingen, J. L., "A Suggested Semi-Empirical Method for the Calculation of the Boundary-Layer Region," Delft, The Netherlands, Rept. No. VTH71, VTH74, 1956.

[9]Narasimha, R., and Dey, J., "Transitional Spot Formation Rate in Two-Dimensional Boundary Layers," *Numerical and Physical Aspects of Aerodynamic Flows III*, edited by T. Cebeci, Springer-Verlag, New York, 1986, pp. 57–74.

[10]Dhawan, S., and Narasimha, R., "Some Properties of Boundary-Layer Flow During the Transition from Laminar to Turbulent Motion," *Journal of Fluid Mechanics*, Vol. 3, 1958, pp. 418–436.

[11]Chen, K. K., and Thyson, N. A., "Extension of Emmons' Spot Theory to Flows on Blunt Bodies," *AIAA Journal*, Vol. 9, 1971, pp. 821–825.

[12]Cebeci, T., Clark, R. W., Chang, K. C., Halsey, N. O., and Lee, K., "Airfoils with Separation and the Resulting Wakes," *Journal of Fluid Mechanics*, Vol. 163, 1986, pp. 323–347.

[13]Cebeci, T., Jau, J., Vitiello, D., and Chang, K. C., "Prediction of Post-Stall Flows on Airfoils," *Numerical and Physical Aspects of Aerodynamic Flows IV*, edited by T. Cebeci, Springer-Verlag, Heidelberg, 1990, pp. 93–106.

[14]Gleyzes, C., Cousteix, J., and Bonnet, J. L., "A Calculation Method of Leading-Edge Separation Bubbles," *Numerical and Physical Aspects of Aerodynamic Flows II*, edited by T. Cebeci, Springer-Verlag, New York, 1984, pp. 173–192.

[15]Drela, M., and Giles, M. B., "Viscous-Inviscid Analysis of Transonic and Low Reynolds Number Airfoils," *AIAA Journal*, Vol. 25, Oct. 1987, pp. 1347–1355.

[16]Walker, G. J., Subroto, P. H., and Platzer, M. F., "Transition Modeling Effects on Viscous/Inviscid Interaction Analysis of Low Reynolds Number Airfoil Flows Involving Laminar Separation Bubbles," American Society of Mechanical Engineers, Paper 88-GT-32, June 1988.

[17]Cebeci, T. "Essential Ingredients of a Method for Low Reynolds-Number Airfoil," *AIAA Journal*, Vol. 27, 1989, p. 1680.

[18]Halsey, N. D., "Potential Flow Analysis of Multielement Airfoils Using Conformal Mapping," *AIAA Journal*, Vol. 17, No. 12, 1979, p. 1281.

[19]Cebeci, T., "Separated Flows and Their Representation by Boundary-Layer Equations," California State Univ., Long Beach, CA, ONR-CR215-234-2, 1976.

[20]Veldman, A. E. P., "New Quasi-Simultaneous Method to Calculate Interacting Boundary Layers," *AIAA Journal*, Vol. 19, 1981, p. 769.

[21]Cebeci, T., and Smith, A. M. O., *Analysis of Turbulent Boundary Layers*, Academic Press, New York, 1974.

[22]Chang, K. C., Bui, M. N., Cebeci, T., and Whitelaw, J. H., "The Calculation of Turbulent Wakes," *AIAA Journal*, Vol. 24, 1986, p. 200.

[23]Cebeci, T., and Egan, D., "Prediction of Transition Due to Isolated Roughness," *AIAA Journal*, Vol. 27, 1989, pp. 870–875.

[24]McGhee, R. J., Jones, G. S., and Jouty, R., "Performance Characteristics from Wind-Tunnel Tests of a Low Reynolds-Number Airfoil," AIAA Paper 88-0607, Jan. 1988.

[25]Gleyzes, C., Cousteix, J., Bonnet, J. L., "Theoretical and Experimental Study of Low Reynolds Number Transitional Separation Bubbles," *Proceedings of the Conference on Low Reynolds Number Airfoil Performance*, edited by T. J. Mueller, UNDASS-CP-778123, June 1985.

[26]Mack, L. M., "Transition and Laminar Instability," Jet Propulsion Laboratory Publication 77-15, 1977.